2021 43rd Annual International Conference of the
IEEE Engineering in Medicine & Biology Society (EMBC)
Oct 31 - Nov 4, 2021. Virtual Conference

Pen-point Trajectory Analysis During Trail Making Test Based on a Time Base Generator Model

Hiroto Sakai[1], *Student Member, IEEE*, Akira Furui[1], *Member, IEEE*, Seiji Hama[2], Akiko Yanagawa[2], Koki Kubo[3], Yutaro Morisako[3], Yuki Orino[3], Maho Hamai[3], Kasumi Fujita[3], Tomohiko Mizuguchi[4], Akihiko Kandori[5], *Senior Member, IEEE*, and Toshio Tsuji[1], *Member, IEEE*

***Abstract*— The Trail Making test (TMT) is a widely used neuropsychological test to assess the cognitive function of patients. This paper presents the analysis method of pen-point trajectory during the TMT based on a time base generator (TBG). In the proposed method, the movement segments between targets are first extracted from pen-point trajectories, which are measured during performance of the TMT on an iPad. By fitting the extracted trajectories with a TBG-based trajectory generation model, the proposed method can then calculate quantitative indices representing the shape and collapse of the velocity profile. In the experiment, we analyzed TMT data from 25 stroke patients who were classified into three groups according to their scores on the Mini-Mental State Examination (MMSE). The results revealed that most of the measured inter-target trajectories had unimodal bell-shaped velocity profiles, as seen in reaching movements. Furthermore, we found that the degree of collapse in the velocity profile shape increased significantly when the cognitive function decreased.**

I. Introduction

Vascular dementia (VaD), which is a form of dementia commonly caused by strokes, can lead to a variety of serious impairments, including aphasia, attention deficit, and executive dysfunction [1]. In particular, it has recently been reported that coronavirus disease 2019 increases the risk of thrombotic complications, such as ischemic stroke, by up to 30% [2]; therefore, the number of patients with VaD is likely to increase in the future. Because early detection of VaD and appropriate rehabilitation can slow down cognitive decline [3], it is important to actively perform cognitive function tests.

The Trail Making Test (TMT) is one of the most widely used tests in neuropsychological assessments as an indicator of attention [4]. In the standard TMT, the patient used a pen to draw lines, in a specified order, between all of targets on a piece of paper; the outcome measure is the time to complete the test. The TMT reflects various cognitive processes in patients, such as visual search and visuoperceptual abilities as well as attention, but in clinical practice, this test is only assessed in terms of its completion time. Consequently, the TMT is non-specific in identifying factors that contribute to cognitive decline [5].

Because the TMT is a test in which the subject connects each of the targets with a line, pen-point movements between any pair of targets can be regarded as a kind of reaching movement towards a given target. Human reaching movements are controlled according to trajectory planning in the brain based on initial position to a target. In particular, proficient reaching movements have invariant characteristics such as a roughly straight path and the symmetrical bell-shaped velocity profile [6]. Ghilardi *et al.* reported that the velocity profile of the hand reaching trajectory collapses in Alzheimer's disease patients [7]. Therefore, quantitative evaluation of the velocity profile characteristics during the TMT may lead to a motor assessment and multifaceted evaluation of the cognitive functions necessary for the performance of the TMT.

As a method for evaluating the shape of the velocity profile during a reaching movement, Kittaka *et al.* proposed a parameterization method [8] for reaching trajectories based on a time base generator (TBG) [9] that can generate an asymmetric bell-shaped velocity profile. In this method, the shape of the velocity profile is represented by model parameters, resulting in the quantitative evaluation.

In this paper, we propose a method to analyze the pen-point trajectories during the TMT based on the TBG model. In the proposed method, the trajectory between each pair of targets is extracted from a series of data points obtained by performing the TMT on an iPad. The model parameters are then estimated by fitting the velocity profile to a TBG-based trajectory generation model, enabling the quantitative evaluation of the shape of the velocity profile. Consequently, we can evaluate the performance of the TMT based on the velocity profile characteristics.

II. Pen-point Trajectory Analysis Method

Fig. 1 shows an overview of the proposed analysis method. In the proposed method, the pen-point trajectory during the TMT is measured on an iPad, and the velocity data are segmented between each pair of targets, to extract the movement segments. The extracted trajectories are then fitted

*This work was not supported by any organization

[1]H. Sakai, A. Furui and T. Tsuji are with the Graduate School of Advanced Science and Engineering, Hiroshima University, Higashi-hiroshima, 739-8527 Japan (e-mail: hirotosakai@hiroshima-u.ac.jp).

[2]S. Hama and A. Yanagawa are with Department of Neurosurgery, Graduate School of Biomedical and Health Science, Hiroshima University, Hiroshima 734-8551, Japan and also with Hibino Hospital, Department of Rehabilitation, Hiroshima, 731-3164 Japan.

[3]K. Kubo, Y. Morisako, Y. Orino, M. Hamai, K. Fujita are with Hibino Hospital, Hiroshima, 731-3164 Japan.

[4]T. Mizuguchi is with Optronics Division, Healthcare Systems Business Promotion Project, Maxell Ltd., Tokyo, Japan.

[5]A. Kandori is with Center for Exploratory Research, Research and Development Group, Hitachi Ltd., 185-8601, Tokyo, Japan.

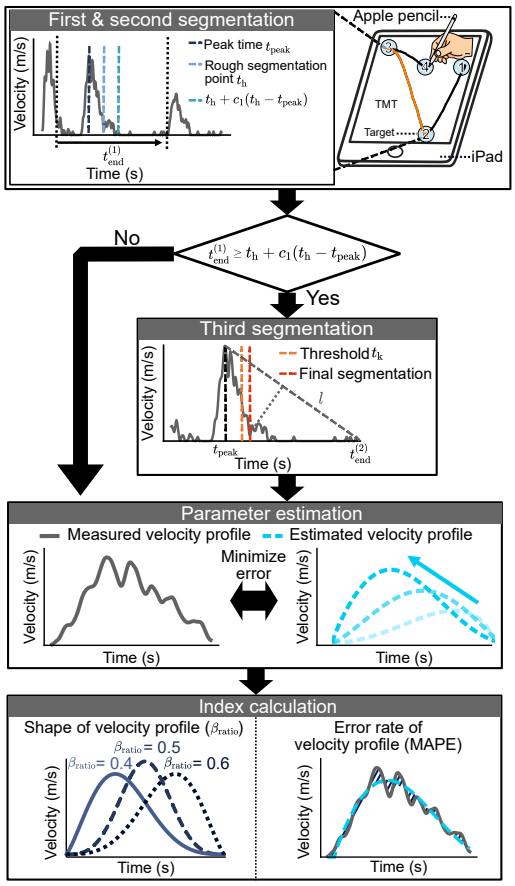

Fig. 1. Overview of the proposed analysis method

with the TBG-based trajectory generation model to evaluate the characteristics of the velocity profile using the model parameters.

A. Segmentation of velocity profile

First, the pen-point position data measured from the iPad are resampled at f_s (Hz) using a cubic spline interpolation, because the sampling frequency of the measured data is not constant. The resampled position data are digitally filtered using a zero-phase-lag second-order Butterworth low-pass filter with a cutoff frequency of f_{low} (Hz), and the tangential velocity and acceleration are calculated. Next, the pen-point trajectory is segmented in the following three steps, (i)–(iii), to extract the movement segments. In the first and second segmentations, the approximate movement duration is determined, and then in the third segmentation, the dwell segment is removed, based on the algorithm proposed by Jackson *et al.* [10].

(i) The trajectory between arbitrary targets is roughly extracted from a series of the trajectory data recorded during the TMT based on the point where the sign of the acceleration changes. We define the peak and end times of the data after the extraction as t_{peak} and $t_{\mathrm{end}}^{(1)}$, respectively.

(ii) In the second segmentation, we first calculate the approximate endpoint of the movement segment, t_h, which is the time after the time of peak velocity when either of the following, (a) or (b), is first satisfied.

(a) The time at which the velocity reaches 5% of the peak velocity [8].

(b) The time when the velocity is less than q% of the peak velocity, v_{peak}, and the acceleration become non-negative for the first time.

In cases where neither of the above conditions is satisfied, $t_{\mathrm{end}}^{(1)}$, as determined by the first segmentation is set to t_h. For the segmentation in step (iii) to be performed stably, the data must contain a certain length of dwell segment. Thus, if the end time $t_{\mathrm{end}}^{(1)}$ is shorter than $t_h + c_1(t_h - t_{\mathrm{peak}})$ (c_1 is an arbitrary coefficient), it is considered insufficient to perform step (iii), and t_h is taken as the final segmentation point without step (iii). Otherwise, $t_h + c_2(t_h - t_{\mathrm{peak}})$ ($c_2 > c_1$ is an arbitrary coefficient) is set as the second segmentation point and the calculations continue with step (iii).

(iii) The threshold t_k is calculated based on a relative distance defined by Jackson *et al.* [10]. The line segment l between $(t_{\mathrm{peak}}, v_{\mathrm{peak}})$ and $(t_{\mathrm{end}}^{(2)}, v_{\mathrm{end}}^{(2)})$ is also defined, where $t_{\mathrm{end}}^{(2)}$ and $v_{\mathrm{end}}^{(2)}$ are the time and velocity at the endpoint of the data after step (ii), respectively. The time after t_k with the largest orthogonal distance between l and the measured velocity profile is set as the final segmentation point (see Fig. 1). Furthermore, the start point of the movement segmentation can also be determined by reversing the time series of the trajectory data and using the same procedure.

By applying the above procedure to all the targets, it is possible to automatically split the dwell and movement segments according to the shape of the velocity profile from the trajectory during the TMT.

B. Modeling of pen-point trajectory based on TBG

This subsection describes the modeling of a pen-point trajectory between each pair of targets during the TMT based on TBG. The TBG is a time function generator capable of generating a bell-shaped velocity profile under a framework of combined feedforward and feedback control [9]. The extended TBG model proposed by Kittaka *et al.* can be applied to the quantification of the velocity profile of the hand trajectory [8].

Let x be the tangential position of the pen-point trajectory in the extracted movement segment, then the extracted velocity $\dot{x}$ can be described as follows:

$$\dot{x} = \underbrace{\alpha\gamma\xi^{\beta_1}(1-\xi)^{\beta_2}}_{=:\hat{\dot{x}}} + \epsilon \tag{1}$$

where $\hat{\dot{x}}$ is the TBG model proposed by Kittaka *et al.* [8] and ϵ represents an error component that cannot be represented by the TBG model. By modeling the pen-point velocities between targets using equation (1), the shape of the bell-shaped velocity profile can be evaluated using the parameters of $\hat{\dot{x}}$, and its collapse can be evaluated using ϵ.

In the TBG model, α represents the target distance, and t_s and t_f represent the start and end times of movements, respectively. In addition, $\xi(t)$ is a TBG that can represent symmetric and asymmetric bell-shaped velocity profiles and satisfies the monotonicity of $\xi(t_s) = 0$, $\xi(t_s + t_f) = 1$, and $\xi = \hat{x}/\alpha$. The parameter β_i $(i = 1, 2)$, that is a positive constant under the $0 < \beta_i < 1$, determines the shape of the velocity profile. The γ as a function of t_f is defined as follows:

$$\gamma = \frac{\Gamma(1-\beta_1)\Gamma(1-\beta_2)}{t_f\Gamma(2-(\beta_1+\beta_2))}. \tag{2}$$

The next subsection outlines a method for the estimation of the model parameters.

C. Parameter estimation

Assuming that N samples of pen-point velocity data $\dot{x}_i$ $(i = 1, \ldots, N)$ are given from the extracted movement segment, the parameters t_s, t_f, β_1, β_2, and α can be estimated by minimizing evaluation function $J = \sum_{i=1}^{N} \rho(\dot{x}_i - \hat{\dot{x}})$ for the predicted value $\hat{\dot{x}}_i$ in the model. Here, $\rho(\cdot)$ is a loss function based on Tukey's biweight estimation method [11]. To minimize the evaluation function, the trust-region reflective (TRF) method was adopted; this is one of the methods for solving nonlinear least-squares problems with bound constraints. After the optimization calculation, let $\dot{x} - \hat{\dot{x}}$ be the ϵ in (1). The model parameters can thus be estimated from the pen-point trajectory measured during the TMT.

D. Index calculation

On the basis of the estimated parameters of equation (1), we calculate indices for quantitatively evaluating the characteristics of the velocity profile. Here, the acceleration of ξ in the model is defined as follows:

$$\ddot{\xi} = \gamma^2 \xi^{2\beta_1 - 1}(1-\xi)^{2\beta_2 - 1}[\beta_1 - (\beta_1 + \beta_2)\xi]. \tag{3}$$

According to this equation, the estimated velocity $\hat{\dot{x}}$ has an absolute maximum value at $\xi = \beta_1/(\beta_1 + \beta_2)$. Kittaka *et al.* defined this as β_{ratio}, which represents the asymmetry of the velocity profile [8].

The collapse of the shape of velocity profiles, which is reported in a previous study [7], cannot be expressed by β_{ratio}. Therefore, we focused on the error term ϵ in equation (1), and computed the mean absolute percentage error (MAPE) with N samples of the measured velocity $\dot{x}_i$ and predicted velocity $\hat{\dot{x}}_i$ as follows:

$$MAPE = \frac{100}{N}\sum_{i=1}^{N}\left(\left|\frac{\epsilon_i}{\dot{x}_i}\right|\right) \tag{4}$$

As described above, we can evaluate the characteristics of the measured velocity profile during the TMT by calculating β_{ratio}, which represents the shape of the velocity profile along the time axis, and MAPE, which represents the degree of collapse of the velocity profile.

III. Experiment

To verify the effectiveness of the proposed method, an experiment was conducted to collect pen-point trajectories during the TMT, and the results analyzed with the proposed method. Fifty patients admitted to Hibino Hospital were asked to performed the TMT Part A (TMT-A) using an iPad Pro (12.9 inch, version 10.2.1, Apple Inc., CA, USA) and Apple Pencil (1st generation, Apple Inc.). In this paper, we analyzed result from 25 patients who met the following criteria: they were right-handed without paralysis, showed no signs of Parkinson's disease or parkinsonism, and were able to finish the TMT-A within the 300-s time limit. The patients were stratified into three groups—non-dementia group, mild cognitive impairment (MCI) group, and dementia group—according to their scores on the Mini-Mental State Examination (MMSE) [12]. This study was conducted under the approval of the ethics committee of Hiroshima University (E-466-3, E-1554-2), and the TMT-A and cognitive function tests were performed on the subjects after obtaining their informed consent. Detailed information on the subjects is provided in Table I.

In the experiment, segmented inter-target trajectories that involve the pen being lifted (i.e., the pen-point leaving the screen) were excluded from the analysis because they violated the standard TMT procedure. In addition, we analyzed the velocity profile v_i $(i = 1, 2, \ldots, N)$ during the movement segments that satisfied all of the following criteria, (1)–(3), to focus on unimodal velocity profiles: those in which the pen-point was almost stationary near targets, and there was no significant loss of velocity while moving (due to a mistake or having lost sight of the target).

(1) The start and endpoints of the extracted velocity were below q% of the peak velocity.
(2) For any point $i \in \{1, 2, \ldots, t_{\mathrm{peak}}\}$, either m times v_i or q% of the peak velocity was greater than the velocity $v_{1:i-1}$, where we now introduce the notation $1 : i-1$ to denote the set $\{1, 2, ..., i-1\}$.
(3) For any point $i \in \{t_{\mathrm{peak}}, t_{\mathrm{peak}} + 1, \ldots, N\}$, either m times v_i or q% of the peak velocity was greater than the velocity $v_{i+1:N}$.

Fig. 2 shows example visualizations of the above criteria. In this paper, the resampling frequency f_s and cutoff frequency f_{low} were set at 500 Hz and 10 Hz, respectively. The arbitrary coefficients were set to $c_1 = 2$, $c_2 = 3$, $m = 2$, and $q = 20$.

First, the linear correlation analysis was conducted between the model parameters and the physical features during the TMT, to check the validity of analyzing the inter-target pen-point trajectories using the proposed trajectory generation model. The analysis included the estimated parameters (model parameter α, the movement convergence time $t_s + t_f$, and the peak velocity time $\hat{t}_{\mathrm{peak}}$ calculated from the model parameter), and the physical measures (the distance traveled, the movement duration, and the peak velocity time). Here, $\hat{t}_{\mathrm{peak}}$ was defined as follows:

$$\hat{t}_{\mathrm{peak}} = t_s + \frac{1}{\gamma}\int_0^{\beta_r} \xi^{-\beta_1}(1-\xi)^{-\beta_2}\mathrm{d}\xi, \tag{5}$$

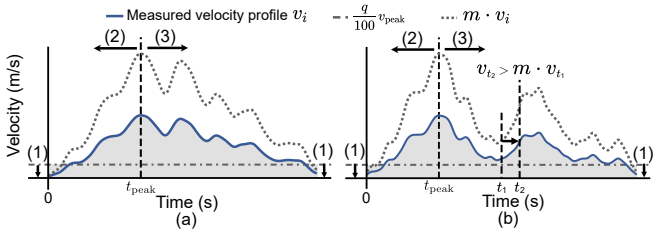

Fig. 2. Examples of visualization of criteria (1)–(3) for unimodal velocity profile. (a) All criteria were satisfied. (b) Criterion (3) was not satisfied because $v_{t_2} > m \cdot v_{t_1}$.

TABLE I
SUBJECT CONDITIONS

Group	Number of patients	Age (years)	MMSE
Non-dementia	13	68.2 ± 7.56	29.5 ± 0.66
MCI	5	76.8 ± 1.10	26.2 ± 1.10
Dementia	7	78.0 ± 15.6	20.7 ± 0.49

MMSE = Mini-mental state examination, MCI = Mild cognitive impaired.

where β_r represents the relative position when the velocity profile reaches its peak, i.e., $\beta_r = \beta_{\text{ratio}}$.

Next, we conducted an analysis to investigate the relationship between the proposed indices obtained and the corresponding cognitive functions. In this analysis, the two evaluation indices of the proposed method, β_{ratio} and MAPE, were calculated for each group of patients (non-dementia, MCI, and dementia) classified according to the MMSE, and the differences between the groups were evaluated.

IV. RESULTS

Of the trajectories between the successive target numbers obtained from the 25 subjects, 88% of the trajectories satisfied the analysis criteria (1)–(3). Fig. 3 shows examples of the measured velocity profiles and estimated velocity profiles obtained with the TBG-based trajectory generation model for each patient group. Fig. 4 shows the relationships between the estimated parameters from the model and the physical features obtained from the measured TMT data. In the figure, Pearson's product-moment correlation coefficients r and corresponding p values based on t-tests are also shown.

Fig. 5 shows the mean values of the estimated velocity profiles and the two evaluation indices calculated by the proposed method. The p-values from the Brunner-Munzel test (significance level: 5%) with the Holm adjustment and effect sizes (Cliff's d) are also shown. The effect size d is a statistical measure of the magnitude of the difference between two sample proportions, with $0.147 \leq d < 0.33$ generally defined as a small effect, $0.33 \leq d < 0.474$ as a moderate effect, and $0.474 \leq d$ as a large effect.

There were significant differences in the mean velocities between all groups. In the MAPE, there were significant differences between the dementia group and the other two groups. However, there were no significant differences in β_{ratio} between any of the cognitive function groups, and the effect size was less than a small effect. Hence, we conducted

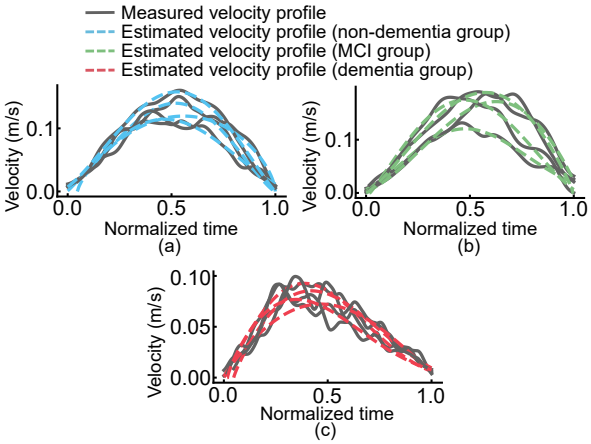

Fig. 3. Examples of measured and estimated velocity profiles. The lines in each graph represent the velocity profiles between targets 18 and 19 for different subjects. (a) Non-dementia group, (b) mild cognitive impairment (MCI) group, and (c) dementia group.

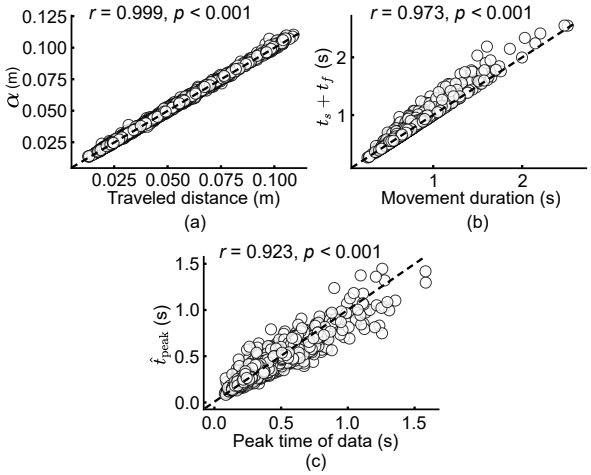

Fig. 4. Scatter plots of the estimated parameters and physical features extracted from the TMT. (a) α and traveled distance. (b) $t_s + t_f$ and movement duration. (c) $\hat{t}_{\text{peak}}$ and peak time of data. Dashed diagonal lines indicate the $y = x$ lines. The correlation coefficients and the corresponding p values based on t-test are also shown.

equivalence tests based on two one-sided tests (TOSTs) with the Holm adjustment for each patient group. The allowable difference in the TOSTs was set to 0.05, which is 5% of the possible range of the β_{ratio}. The TOSTs confirmed that β_{ratio} was significantly equivalent in all cognitive function groups ($p < 0.001$).

V. DISCUSSION

In this study, we analyzed the movements in connecting targets during the TMT. As a result, nearly 90% of the trajectories obtained during the TMT satisfied the analysis criteria (1)–(3). This means that most of the pen-point in the extracted movement segments move toward the target with a unimodal velocity profile. Previous studies have suggested that complex upper limb movements such as handwriting can be represented by a combination of simple reaching movements [8], [13]. We revealed that the movements to connect targets during the TMT had similar characteristics to reaching movements.

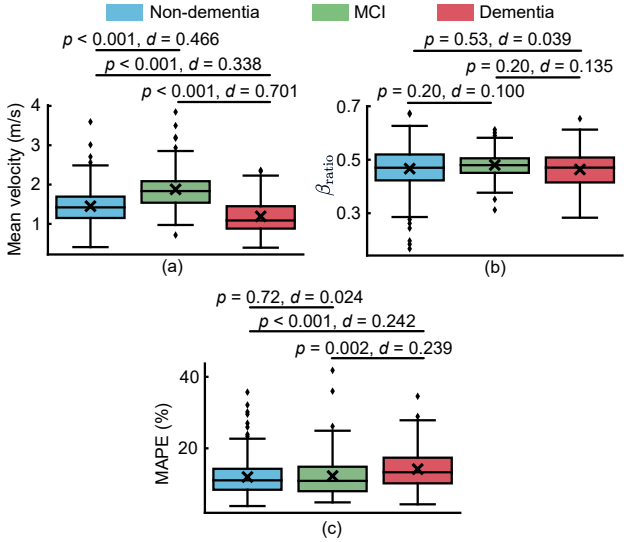

Fig. 5. Box plots of evaluation indices for each patient group. (a) Estimated mean velocity with normalized movement distance. (b) β_{ratio}. (c) Mean absolute percentage error (MAPE). The mark $\times$ in the box plots denote the mean values for each patient group. The p values from the Brunner-Munzel test and the effect size d are also shown.

In Fig. 3, the examples of the fitting results indicated that the proposed TBG-based model was appropriately fitted to the velocity profiles in the movement segments obtained from a series of data during the TMT. In addition, the correlation coefficients between the physical features and estimated parameters were significantly higher than 0.9 for all the combinations (Fig. 4). These results suggest that the physical features in the TMT can be quantitatively evaluated using the model parameters. Therefore, the validity of applying the TBG-based model to velocity profiles during the TMT was demonstrated.

The index β_{ratio}, which represents the degree of symmetry of a bell-shaped velocity profile, was significantly equivalent for each group. However, the mean value of the estimated velocity in the dementia group was significantly slower than that in the other groups (Fig. 5(a)). Fitts reported that human arm movement has a trade-off between speed and accuracy [14]. Therefore, patients in the dementia group may maintain the accuracy of their movements by slowing down the pen-point speed, resulting in the same shape of velocity profile as seen for the patients without dementia.

In the dementia group, the MAPE, which indicates the degree of collapse of the shape of the velocity profile, was significantly larger than in the others (Fig. 5(c)). Similarly, Ghilardi *et al.* reported that the reaching movements of patients with Alzheimer's disease were slow, with a collapse of the velocity profile [7]. They suggested that this collapse may be due to the fact that the patients with Alzheimer's disease who have severe dementia modify their trajectories sequentially, according to visual feedback in addition to the results of feedforward motor planning. Therefore, the increase in MAPE observed in the dementia group may indicate that the feedforward motor planning in the dementia group could not be properly reflected in their movements, and the trajectory was mainly adjusted by visual feedback.

VI. Conclusion

In this paper, we proposed a method to analyze the pen-point trajectory during the TMT using the TBG-based trajectory generation model. In the proposed method, a three-step segmentation process is applied to the pen-point trajectories obtained from the TMT on the iPad to extract the movement segments showing unimodal velocity profiles. Furthermore, the proposed method can quantitatively evaluate the characteristics of the velocity profile by fitting the extracted velocity profile based on the TBG model.

The experiment indicated that the movements during the TMT can be quantitatively evaluated based on the TBG model. Furthermore, we revealed that the degree of symmetry of the velocity profiles was statistically equivalent regardless of cognitive function, whereas the degree of collapse of the velocity profile significantly increased when cognitive function decreased.

In the future, we may also assess the cognitive function necessary for the performance of the TMT, by evaluating the shape of the pen-point trajectories and vibration-like error components, in addition to the shape of the velocity profile. Therefore, we plan to analyze the linearity of trajectories and the frequency characteristics of the noise term ϵ.

References

[1] R. N. Kalaria, R. Akinyemi, and M. Ihara, "Stroke injury, cognitive impairment and vascular dementia," *Biochim. Biophys. Acta, Mol. Basis Dis.*, vol. 1862, no. 5, pp. 915–925, 2016.

[2] F. Klok *et al.*, "Incidence of thrombotic complications in critically ill ICU patients with COVID-19," *Thromb. Res.*, vol. 191, pp. 145–147, 2020.

[3] S. T. Pendlebury, "Dementia in patients hospitalized with stroke: Rates, time course, and clinico-pathologic factors," *Int. J. Stroke*, vol. 7, no. 7, pp. 570–581, 2012.

[4] R. M. Reitan, "The relation of the trail making test to organic brain damage." *J. Consult. Psychol*, vol. 19, no. 5, p. 393, 1955.

[5] S. F. Crowe, "The differential contribution of mental tracking, cognitive flexibility, visual search, and motor speed to performance on parts A and B of the trail making test," *J. Clin. Psychol.*, vol. 54, no. 5, pp. 585–591, 1998.

[6] P. Morasso, "Spatial control of arm movements," *Exp. Brain Res.*, vol. 42, no. 2, pp. 223–227, 1981.

[7] M. F. Ghilardi *et al.*, "Visual feedback has differential effects on reaching movements in Parkinson's and Alzheimer's disease," *Brain Res.*, vol. 876, no. 1-2, pp. 112–123, 2000.

[8] M. Kittaka *et al.*, "Spatiotemporal parameterization of human reaching movements based on time base generator," *IEEE Access*, vol. 8, pp. 104 944–104 955, 2020.

[9] T. Tsuji, Y. Tanaka, and M. Kaneko, "Bio-mimetic trajectory generation based on human arm movements with a nonholonomic constraint," *IEEE Trans. Syst. Man Cybern. Syst.*, vol. 32, no. 6, pp. 773–779, 2002.

[10] K. Jackson *et al.*, "Characterizing functional upper extremity movement in haptic virtual environments," in *Proc. 42th Annu. Int. Conf. IEEE Eng. Med. Biol. Soc.*, 2020, pp. 3166–3169.

[11] A. E. Beaton and J. W. Tukey, "Fitting of power series, meaning polynomials, illustrated on band-spectroscopic data." *Technometrics*, vol. 16, no. 2, pp. 147–185, 1974.

[12] M. F. Folstein, S. E. Folstein, and P. R. Mchugh, ""Mini-mental state": a practical method for grading the cognitive state of patients for the clinician," *J. Psychiatr. Res.*, vol. 12, no. 3, pp. 189–198, 1975.

[13] J. G. V. Miranda *et al.*, "Complex upper-limb movements are generated by combining motor primitives that scale with the movement size," *Sci. Rep.*, vol. 8, no. 1, p. 12918, 2018.

[14] P. M. Fitts, "The information capacity of the human motor system in controlling the amplitude of movement," *J. Exp. Psychol.*, vol. 47, no. 6, pp. 381–391, 1954.